RSC Advances

ROYAL SOCIETY OF CHEMISTRY

www.rsc.org/advances

Cite this: DOI: 10.1039/c0xx00000x

www.rsc.org/xxxxxx

ARTICLE TYPE

An Approach towards Synthesis and Characterization of ZnO@Ag Core@shell Nanoparticles in Water-in-Oil Microemulsion

Shazia Sharmin Satter[a], Mahfuzul Hoque[a], M. Muhibur Rahman[b], M. Yousuf A Mollah[a], Md. Abu Bin Hasan Susan[a]*

Received (in XXX, XXX) Xth XXXXXXXXX 20XX, Accepted Xth XXXXXXXXX 20XX
DOI: 10.1039/b000000x

Water-in-oil microemulsions have been found to be good templates and suitable media for synthesis of ZnO and ZnO@Ag nanoparticles to offer themselves as ideal 'nanoreactors' for uniform fabrication of core@shell nanoparticles.

Semiconducting core@metal shell nanoparticles have been one of the most fascinating materials of the modern age and the preparation, characterization and fabrication of materials of this variety has received an upsurge of interest. Such nanohybrid particles are expected to colossally contribute to the modern scientific world due *inter alia,* their ability to integrate multifunctional characteristics in one system. For instance, ZnO@Ag core@shell nanoparticles exhibit antibacterial activity[1a] and promising characteristics for photoelectrical devices[1b] and photoelectrochemical anode materials[1c].

ZnO is a semiconductor with a wide band-gap and possesses enhanced optical and electrical properties, electrochemical stability and high electron mobility in nano-level. Silver on the other hand is considered to be a noble metal with remarkable catalytic activity, non-toxicity, cost-effectiveness and shows antibacterial activity. Excellent characteristics together with low-cost prompted many researchers to prepare ZnO nanoparticles following a wide variety of methods. Direct synthesis of ZnO nanoparticles by basic hydrolysis of zinc nitrate in water-in-oil microemulsion (w/o)[2a] is a notable example. With a view to enhancing properties of ZnO nanoparticles, Wang and co-workers reported preparation of ZnO-based core@shell nanoparticles in reverse micelles where SiO_2 core was coated with ZnO shell[2b] and ZnO based core@shell nanotubes and nanorods have been synthesized electrochemically[2c]. There have also been several attempts to fabricate ZnO both as core and shell as in ZnO@Ag core@shell and Ag@ZnO core@shell nanoparticles. The crystalline mismatch between ZnO and silver places a stumbling block on the fabrication of ZnO@Ag or Ag@ZnO core@shell nanoparticles. ZnO in crystalline form is hexagonal cubic packed (HCP) whereas, silver is face centered cubic (FCC). Synthesis of ZnO microspheres coated with silver nanoparticles[3a] and ZnO nanorods coated with silver[3b] were reported earlier where attachment of silver on surface of ZnO was described to be correlated with the presence of selective and suitable surface[3a,b]. Pacholski et al carried out site-specific deposition of silver nanoparticles onto ZnO nanorods by a photocatalytic wet chemical method where silver nanoparticles were located at one end of ZnO nanorods due to the crystalline mismatch[3c]. This phenomenon is known as 'rattle'. Noble silver nanoparticles were decorated with ZnO; but due to the difference in crystalline structure, large number of silver nanoparticles remained in final products, unattached since it was difficult to avoid self-nucleation and the core@shell formed was dumbell-shaped rather than a spherical one [3d,e,f]. Despite several reports, a systematic approach to uniformly coat silver nanoparticles on ZnO in a controllable manner or vice versa remains a sombre challenge.

The 'water-in-oil' (w/o) microemulsions can be reckoned as true nanoreactors containing "water pools" and offer the potential to control dimension of nanoparticles[4]. In this work, we report our approach towards preparation of heterostructured nanoparticles in w/o microemulsion and show evidences that uniform coating of silver can be successfully performed on ZnO nanoparticles and the properties may be systematically tuned by varying the thickness of the core and the shell. Direct synthesis of ZnO@Ag core@shell nanoparticles have been carried out for the first time using a double scheme microemulsion method and the limiting factor of crystalline mismatch has been successfully overcome.

Triton X-100 and cyclohexane (Sigma Aldrich) were used as surfactant and oil phase, respectively for preparation of w/o microemulsions. Hexanol (Sigma Aldrich) was used as a co-surfactant which eventually acted as an 'anchor' and hence played an important role for the stabilization of microemulsion. 0.25 mol dm^{-3} of TX-100 solution was prepared in hexanol/cyclohexane and a molar ratio of 1:4 of TX-100: hexanol was maintained. Equal volumes of microemulsions were taken in two stoppered vials. 40 µL of 0.1mol dm^{-3} $Zn(NO_3)_2$ (Riedel De Haenag Seelze Hannover) was incorporated in one microemulsion, and was mixed with another microemulsion with 80 µL of 1 mol dm^{-3} NH_4OH (Merck) incorporated in it. The mixture was shaken until a transparent microemulsion was obtained. The resultant mixture was then kept overnight. The w/o microemulsion containing the 0.42 mmol dm^{-3} of $AgNO_3$ (Merck) with respect to the total microemulsion volume was then transferred to a vial containing ZnO nanoparticles synthesized in w/o microemulsion followed by addition of $NaBH_4$ incorporated in an equal volume of microemulsion of TX-100. Dark brown

Cite this: DOI: 10.1039/c0xx00000x

www.rsc.org/xxxxxx

ARTICLE TYPE

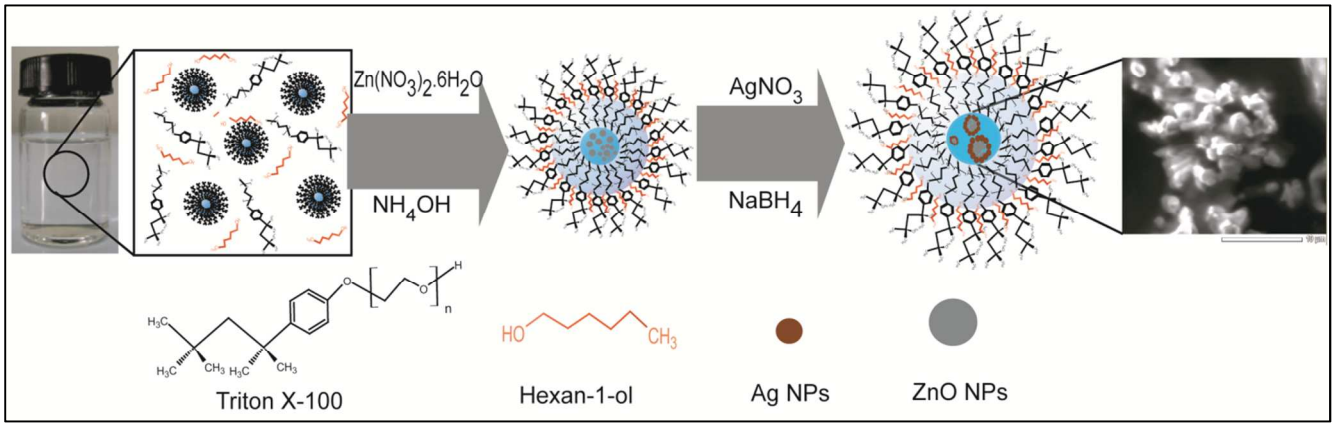

Scheme 1: Synthesis of ZnO@Ag core@shell nanoparticles synthesized in the water pool of w/o microemulsions.

solution was formed which faded with time and thus gave a reddish brown coloured solution. Scheme 1 shows the overall representation of the synthesis of the core@shell nanoparticles in w/o microemulsion.

The water to surfactant molar ratio (W_o) was maintained constant at 13.34. Under the highly basic condition, $[Zn(OH)_4]^{2-}$ ions formed (due to basic hydrolysis of zinc nitrate precursor) easily in the water pools of w/o microemulsion was converted to ZnO since the coordination state of $Zn^{2+}$and O^{2-} is considerably similar in both ZnO and $[Zn(OH)_4]^{2-}$ [5]. The *in situ* reduction of $Ag(NO_3)_2$ resulted in the production of silver which *via* the process of nucleation deposited as a layer of silver on ZnO nanoparticles.

FTIR spectrum was recorded over a range of 1000-400 cm^{-1} (*cf.* Fig.S1 ES†) to confirm the synthesis of ZnO nanoparticles. A band at around 555 cm^{-1} is assigned to Zn-O stretching and hence confirmed the presence of ZnO[6a]. The band appearing at 522 cm^{-1} can also be considered as a characteristic peak of ZnO. However, peaks split at 522 cm^{-1} and 555 cm^{-1}, which might be the result of the stretching polarity of the Zn-O bands and aggregation of nanoparticles[6b]. XRD measurement of the ZnO nanoparticles as well as ZnO@Ag core@shell nanoparticles (centrifuged from microemulsions and calcined at 250 ^oC) was carried out (*cf.* Fig.S2 (a) and (b) ES†). All the diffraction lines in X-ray powdered pattern are perfectly indexed as hexagonal cubic packed structure of ZnO (*cf.* Fig.S2 (a) ES†). The peaks show the single phase formation of ZnO nanoparticles with absence of any impurities[2a]. Four additional, weak peaks are observed (*cf.* Fig.S2 (b) ES†) which can be assigned to the (111), (200), (311) and (222) crystal planes of face-centered cubic (fcc) structure of Ag crystallite[3a]. The peaks for bare ZnO and ZnO of the core@shell nanoparticles are intense showing higher degree of crystallinity and those of the silver shell are weak due to thin coating of silver. EDX spectra correspond to the total area shown in (Fig 1) which confirm the presence of the elements Zn, O and Zn, O and Ag in ZnO and ZnO@Ag core@shell nanoparticles prepared from microemulsions with W_o=13.34, respectively (*cf.* Fig.S3(a) and S3(b) ES†). When spotted on the dark portion, peaks are shown for Zn and O and when spotted on the brighter region, peaks for Ag appear along with Zn and O which suggests that silver nanoparticles are present along with ZnO (Fig.S3(b) ES†). The peak corresponding to carbon originated from the sample support as well as from carbon containing TX-100.

From the SEM image (model: JEOL JSM-6490LA) of ZnO@Ag core@shell nanoparticles formed in w/o microemulsion with W_o= 13.34 it is clear that the core@shell nanoparticles formed are nearly spherical in shape (Fig.1). Magnification of a selected part reveals two distinct regions; the inner dark part and a shiny portion surrounding the dark region. This indicates the formation of a very thin layer of metallic silver around the semiconducting ZnO core.

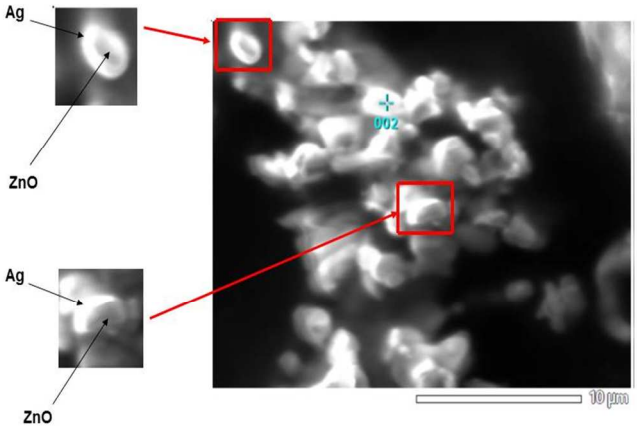

Fig.1 SEM image of ZnO@Ag core@shell nanoparticles synthesized at W_o= 13.34.

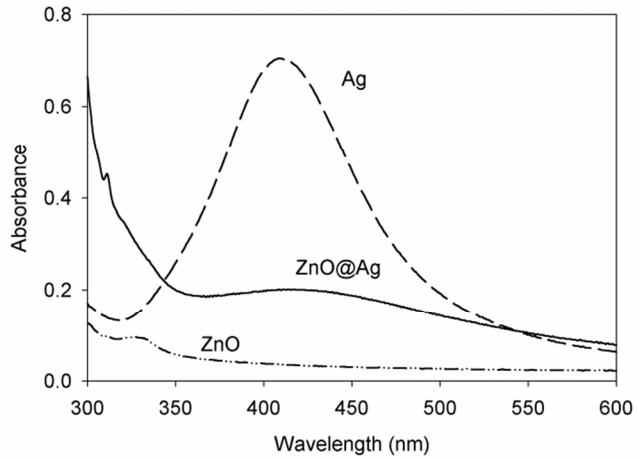

Fig.2 Absorbance spectra of (a) ZnO, (b) Ag and (c) ZnO@Ag core@shell nanoparticle synthesized in w/o microemulsion of TX-100/hexanol/cyclohexane/water at W_o=13.34.

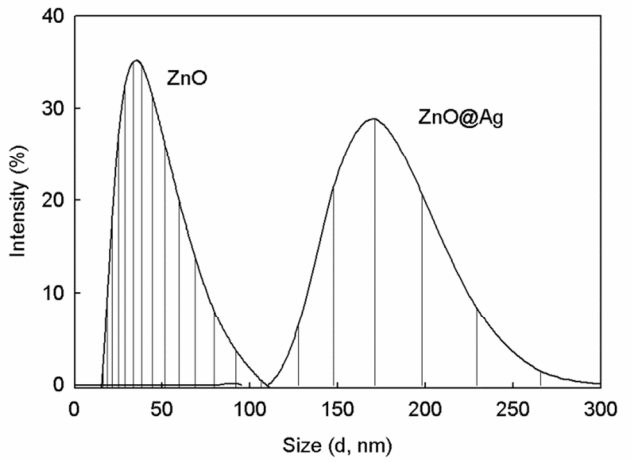

Fig.3 Size distribution of ZnO and ZnO@Ag core@shell nanoparticles synthesized in TX-100/hexanol/cyclohexane w/o microemulsion at W_o=13.34.

The absorbance spectra of ZnO, silver and ZnO@Ag core@shell nanoparticles synthesized at W_o= 13.34 were recorded (Fig 2). The absorption maximum at 326 nm is attributed to the absorption of ZnO nanoparticles. The surface plasmon resonance (SPR) of ZnO@Ag core@shell nanoparticles is shifted to longer wavelength i.e. 420 nm (bathochromic shift) compared to the plasmon resonance of silver nanoparticles showing absorption maximum at 408 nm. Interfacial coupling between silver nanoparticles may be the reason for the broadening and red shift of the surface plasmon absorption[7a].

For coated nanoparticles, plasmon peak position, $\lambda_{peak}{}^2$ is determined by[7b],

$$\frac{\lambda_{peak}{}^2}{\lambda^2} = \epsilon^{\infty} + 2\,\epsilon_m + \frac{2g(\epsilon_s - \epsilon_m)}{3}$$

where, ϵ_s is the dielectric function of shell layer, ϵ_m is the dielectric function of medium i.e. cyclohexane (the w/o microemulsion mostly comprises cyclohexane), g is the volume fraction of shell layer.

The refractive index and dielectric function is related by, $n_s = \epsilon_s{}^{1/2}$

$$\lambda_{peak} = \lambda[\epsilon^{\infty} + 2n^2_{cyclohexane} + \frac{2g(2n^2_{Ag} - 2n^2_{cyclohexane})}{3}]^{1/2}$$

where bulk plasma wavelength, $\lambda = [\frac{4\pi^2 c^2 m_{eff}\epsilon_o}{Ne^2}]^{1/2}$

m_{eff} is the effective mass of free electron of the metal, N is the electron density of the metal.

$$n_{Ag} = 1.07 < n_{cyclohexane} = 1.43248$$

Although refractive index of silver is less than that of cyclohexane, calculation shows that λ_{peak} is greater than λ thus showing a red shift.

If the particles are well separated (thick coating), the dipole-dipole coupling is fully suppressed and the plasmon band is located nearly at the same position of the individual metal particles. In this case, it can be presumed that thin shell of silver has been formed. The ZnO nanoparticles synthesized in w/o microemulsion were kept overnight and silver core was formed after one day. Therefore, the polydispersity of the ZnO nanoparticles might have increased thus showing such a broad peak for the core@shell nanoparticles formed which is near the SPR of silver nanoparticles. The work function of ZnO is more than that of silver (Fig.S4 ES†) and it is noticed that Fermi level of Ag [$E_{f(Ag)}$] is more than that of ZnO [$E_{f(ZnO)}$] which results in the transfer of electrons from silver to ZnO until a new Fermi energy level (E_f) is formed in order to attain equilibration. The electron transfer from silver to ZnO enhances charge separation, which results in the deficiency of electrons on silver nanocrystals. Hence there is a shift in wavelength towards higher value[8].

DLS measurements of the reverse micelles in w/o microemulsion, and ZnO and ZnO@Ag core@shell in reverse micelles were carried out (*cf.* Fig.S5 ES† and Fig.3 respectively). The size of the reverse micelle of the TX-100 microemulsion is 5 ± 1 nm which enables us to reckon them as nanoreactors (*c.f.* Fig.S5 ES†). The sizes of ZnO nanoparticles are 43 ± 2 nm and that of the core@shell nanoparticles are 181 ± 8 nm (Fig.3). The size and particles size distribution (PSD) have been found to increase significantly in case of ZnO@Ag core@shell nanoparticles as compared to that of ZnO nanoparticles. The size and PSD of the core@shell nanoparticles found by DLS measurement (181 ± 8 nm) is also supported by the size found from the Field emission scanning electron microscope (FESEM) (model: JEOL 7600F) micrographs (159 ± 22 nm) (*cf.* Fig.S6(a) and (b)). Under different accelerating voltage (10 kV and 15 kV), FESEM micrographs reveal the sizes and PSD of both the core (100 ± 16 nm) and shell (55 ± 15 nm). From FESEM micrographs of a particular area, sizes of nanoparticles at a definite position are seen to range from 100 nm to 216 nm in which core size ranges from 58 nm to 173 nm and shell thickness ranges from 25 nm to 102 nm.

Since the precursor salts of zinc and silver used are both water soluble, basic hydrolysis of Zn^{2+} and reduction of Ag^{+} occur in the hydrophilic water pool of the nanoreactors. Both ZnO and the silver nanoparticles remain confined in the hydrophilic core which is said to contain water of special properties, such as lower micropolarity, altered nucleophilicity and viscosity to make it a medium different from ordinary water[9a] and water is said to

exhibit major changes from bulk behaviour when $W_o < 20$[9b]. More energy is required for silver to undergo free nucleation. However, in these confined water pools of the reverse micelle which has a 'cage-like' effect, Gibbs energy required is lower for silver nanoparticles to undergo heterogeneous nucleation on the surface of ZnO nanoparticles. The surface of ZnO nanoparticles might have numerous defects and were thermodynamically unstable. Surface reconstruction would further decrease their energy and thus provide active site for heterogenous nucleation and growth of silver nanoparticles.

It is interesting that even after the mismatch, silver nanoparticles are forced to form a layer around the ZnO nanoparticles and hence result in the formation of ZnO@Ag core@shell nanoparticles.

Conclusions

In conclusion, we have established a methodology for the synthesis of ZnO nanoparticles coated uniformly with thin silver nanoparticles in w/o microemulsion of TX-100/hexanol/cyclohexane. The work is now underway to prepare ZnO@Ag core@shell nanoparticles with a wide variation in the thickness of the core and the shell by systematic variation of the constituents and composition of the microemulsions and the concentration of the precursors. The w/o microemulsion system is cost effective and provides a very easy and convenient means to the controllable synthesis of core@shell nanoparticles for tunable optical, electrical, electronic and antimicrobial properties. This may open up a new route for preparing core@shell nanoparticles overcoming the crystalline mismatch and be used to systematically tune properties for task-specific applications.

Notes and references

[a]*Department of Chemistry and Centre for Advanced Research in Sciences, University of Dhaka, Dhaka 1000, Bangladesh. Fax: 88028615583; Tel: 880 2 9661920 Ext. 7162; E-mail: susan@du.ac.bd*

[b]*University Grants Commission of Bangladesh, Agargaon, Dhaka 1207, Bangladesh. Fax: 8802 8181615; Tel: 880 2 8181625; E-mail: mmrahmanugc@gmail.com*

† Electronic Supplementary Information (ESI) available: FTIR, XRD and EDX spectra, Energy band gap structure, DLS data, FESEM micrograph and XRD instrumentation. See DOI: 10.1039/b000000x/

References

1 (*a)* S. Ghosh, V. S. Goudar, K. G. Padmalekha, S. V. Bhat, S. S. Indi, H. N. Vasan, RSC Advances, 2012, **2**, 930; *(b)* T. Wang, Z. Jiao, T. Chen, Y. Li, W. Ren, S. Lin, G. Lu, J. Ye, Y. Bi, Nanoscale, 2013, **5**, 7552; *(c)* Y. Wei, J. Kong, L. Yang, L. Ke, H. R. Tan, H. Liu, Y. Huang, X. W. Sun, X. Lu, H. Du, J. Mater. Chem. A, 2013, **1**, 5045.

2 *(a)* D. Sarkar, S. Tikku, V. Thapar, R. S. Srinivasa, K. C. Khilar, Colloids and Surfaces A: Physicochem. Eng. Aspects, 2011, **381**, 123; *(b)* J.Wang, T Tsuzuki, L Sun, X Wang, *ACS Appl. Mater.* Interfaces, 2010, **2**, 957; (c) Z. L. Wang, R. Guo, G. R. Li, L. X. Ding, Y. N. Ou, Y. X. Tong, RSC Advances, 2011, **1,** 48.

3 *(a)* F. Li, J. Wua, Q. Qin, Z. Li, X. Huang, Superla. Micro., 2010, **47**, 232; *(b)* F. Li,Y. Yuana, J. Luoa, Q. Qina, J. Wua, Z. Li, X. Huang, App. Surf. Sci., 2010, **256**, 6076; *(c)* C. Pacholski, A. Kornowski, H. Weller, Angew. Chem. Int. Ed., 2004, **43**, 4774; *(d)* G. Shan, L. Xu, G. Wang, Y. Liu, J. Phys. Chem. C, 2007, **111**, 3290; *(e)* M. K. Lee, T. G. Kim, W. Kim, Y. M. Sung, J. Phys. Chem. C, 2008, **112**, 10079; *(f)* R. Georgekutty, M. K. Seery, S. C. Pillai, J. Phys. Chem. C, 2008, **112**, 13563.

4 *(a)* S. Hossain, U. K. Fatema, M. Y. A. Mollah, M. M. Rahman, M. A. B. H. Susan, J. Bangladesh Chem. Soc., 2012, **25**, 71; *(b)* S. Sultana, S. Saha, M. M. Islam, M. M. Rahman, M. Y. A. Mollah, M. A. B. H. Susan, J. Electrochem. Soc., 2013, **160**, D524; *(c)* M. A. Haque, M. M. Rahman, M. A. B. H. Susan, J. Solution Chem., 2012, **41**, 447; *(d)* T. I. Mredha, C. K. Roy, M. Y. A. M. Mollah, M. A. B. H. Susan, Electrochim. Acta, 2013, **97**, 231; *(e)* T. Afrin, S. N. Karabi, M. M. Rahman, M. Y. A. M. Mollah, M. A. B. H. Susan, J. Solution Chem., 2013, **42**, 1488; *(f)* J. J. Keya, M. M. Islam, M. M. Rahman, M. Y. A. M. Rahman, M. A. B. H. Susan, J. Electroanal. Chem., 2014, **712**, 161

5 W. J. Li, E. W. Shi, W. Z. Zhong, Z. W. Yin, J. Crys. Growth, 1999, **203**, 186.

6 *(a)* N. Nasakumar, J. B. B. Rayappan, J. App. Sci., 2012, **12,** 1758; *(b)* G. Shan, L. Xu, G. Wang, Y. Liu, J. Phys. Chem. C, 2007, **111**, 3290.

7 *(a)* G. Shan, S. Zheng, S. Chen, Y. Chen, Y. Liu, Colloids. Surf. B:Biointerf., 2012, **94**, 157; *(b)* A. C. Templeton, J. J. Pietron, R.W. Murray, P. Mulvaney, J. Phys. Chem. B, 2000, **104**, 564.

8 G. Shan, L. Xu, G. Wang, Y. Liu, J. Phys. Chem. C, 2007, **111**, 3290.

9 *(a)* P. L. Luisi, B. E. Straube (Eds), Reverse Micelles, Plenum, New York, 1984; *(b)* I. R. Piletic, D. E. Moilanen, D. B. Spry, N. E. Levinger, M. D. Fayer, J. Phys. Chem. A, 2006, **110**, 4985.

Cite this: DOI: 10.1039/c0xx00000x

www.rsc.org/xxxxxx

ARTICLE TYPE

Graphical Abstract